Structural Simulation of Transcatheter Heart Valve in Transcatheter Heart Valve

R. Scuoppo[1], S. Cannata[2], C. Gandolfo[2], and S. Pasta[1,3]
[1]*Dipartimento di Ingegneria, viale delle Scienze Ed.8, University of Palermo, Italy*
[2]*Interventional Cardiology Unit, IRCCS ISMETT via Tricomi, 5, Italy*
[3]*Department of Research, IRCCS ISMETT via Tricomi, 5, Italy*

***Abstract*— The durability of transcatheter heart valves (TAV) remains the main disadvantage of transcatheter heart valve implantation (TAVI) for treating aortic valve stenosis. In this study, we assessed the structural mechanics of TAV-in-TAVI using patient-specific modeling. A parametric analysis highlighted that the outcome of TAV-in-TAV depends on the implanted device position and the planned device to be implanted. Contact pressure evinced the impact of different implantation depth and device size on the TAV-in-TAV. This study may bring new insight in the biomechanical performance of TAV to evaluate options for future interventions when the current TAVs experience device failure.**

***Keywords*—finite-element analysis, transcatheter heart valves, redo-TAVI**

I. Introduction

Transcatheter aortic valve implantation (TAVI) is increasingly used to treat patients with severe aortic (AS) stenosis who are deemed inoperable or at high risk for surgical aortic valve repair [1]. After the publication of positive outcomes in inoperable patients with conventional surgery and in operable patients at high surgical risk, TAVI was included for the first time in the 2012 ESC/EACTS (European Society of Cardiology/European Association for Cardio-Thoracic Surgery) guidelines [2]. These guidelines specifically recommend TAVI for inoperable patients with severe symptomatic AS. Ongoing clinal trials are investigating the feasibility and safety of TAVI in low-risk patients and bicuspid aortic valve as these conditions were considered exclusion criteria in past trials [3].

Transcatheter heart valve (TAV) employed in TAVI is typically comprised of a biological valve mounted on a metal stent frame. The balloon-expandable SAPIEN 3 Ultra device (Edwards, Lifescience, Inc., Irvine, CA, USA) is composed of a metal stent in chrome-cobalt alloy, skirt in polyethylene terephthalate, three valve leaflets made of bovine pericardium, while the Evolut (Medtronic, Minneapolis, MN, USA) is made of porcine pericardium, and mounted on a self-expandable nitinol stent frame and sealing skirt [4].

An increasing number of younger patients with longer life-expectancy receive transcatheter aortic valve implantation (TAVI). Thus, even in the absence of concerns about TAV durability, a substantial proportion of contemporary TAVI patients are expected to live sufficiently long to experience the degeneration and failure of TAV. Indeed, the key disadvantage of TAVs is the limited durability as the chemically treated valve leaflets are not immune to structural degeneration from calcification and thrombosis. For instance, thrombosis was occurred within 3-year from TAVI procedure. The therapeutic option for the treatment of structural TAV degeneration are limited to open-heart surgery and redo-TAVI (or TAV-in-TAV) [5]. While the feasibility of TAV-in-TAV was recently demonstrated, the risk of coronary obstruction due to sinus sequestration is high [6].

In this context, computational modelling may allow to determine the biomechanical interaction of redo-TAVI. This study aimed to develop a computational framework to simulate TAV-in-TAV as clinically performed in one patient with early failure of the implanted device. Patient-specific computational modelling was carried out to determine structural metrics of delivered devices while a parametric analysis of the implantation depth of the second TAVI procedure was performed to assess the impact of the relative device position.

II. Materials and Methods

A. Patient Study Case

A 68-years old gentleman with severe AS was initially treated with a 23-mm SAPIEN 3 Ultra TAV at IRCCS ISMETT in 2019. After 3-year from TAVI, the device failure was treated by redo-TAVI with a 29-mm Evolut Pro device. The patient was discharged and is currently monitored with echocardiography. CT imaging was performed prior the first TAVI procedure for annulus size evaluation, after the TAVI and redo-TAVI.

B. 3D Reconstruction

Pre-TAVI CT images were processed in Mimics (v.21, Materialize, Belgium) to reconstruct the aortic root anatomy and calcific plaques using semi-automatic thresholding of the contrast-enhanced images [7]. Once segmented regions were obtained, the aortic wall and calcific plaques were exported as stereolithographic files for meshing. Since native valve leaflet were not clearly visible at CT scan, a parametric modelling approach was adopted generate the leaflet geometry using anatomic measurements and the CAD tool Rhinoceros (Rhinoceros v.7, McNeel & associates, USA). In brief, two 3rd-order NURBS curves interpolating commissures were delineated to model the free edge of valve leaflets, while the belly of each leaflet was considered using one control points. To model the leaflet-to-sinus attachments, a second set of 3rd-order NURBS curves were developed using Rhino software (v.7.1, McNeel & associates, USA). The NURBS curves were constrained to the aortic root surface by curve-to-surface projection, and then native valve leaflets were developed by a

multi-patch network of NURBS surfaces [8, 9]

Using ICEM meshing software (v2021, ANSYS Inc., USA), the aortic root luminal surface was discretized with unstructured triangular shell elements with size of 0.6 mm. Calcifications were meshed with tetrahedral solid elements with size of 0.5 mm. Native valve leaflets were initially discretized with triangular shell elements (element size of 0.6 mm) and then solid elements were obtained by element protrusion with thickness of 0.5 mm and 4 layers. Figure 1 shows the anatomic model parts of the patient model.

For the sake of simplicity, neo-Hookean models were adopted for both the aortic valve and native valve leaflets. Specifically, the aortic root had C1=1.05 MPa and D=0.048 MPa^{-1} while the AS valve had C1=2.29 MPa and D=0.022 MPa^{-1}[10, 11]. The calcification had a linear-elastic model with Young modulus of 400 MPa and Poisson coefficient of 0.475 [12]. Tie contact conditions were used to constraint anatomic parts while the proximal and distal ends of the aortic root was fixed in all directions.

C. *TAV Models*

Geometrical models of 23-mm SAPIEN 3 Ultra and 29-mm Evolut PRO device frames were obtained by reverse engineering of micro-CT images as described in a previous study from our group [13]. For the 23-mm SAPIEN 3 device, the metallic frame was meshed with nearly 60,000 structured-hexahedral solid elements with reduced integration (C3D8R). The Cobalt-Chromium alloy of stent frame was modeled with Von Mises plasticity and isotropic hardening [12]. The Evolut Pro device was meshed with 315,653 structured-hexahedral solid elements with reduced integration and hourglass control. The stent frame was modelled with nitinol alloy material properties as proposed by Auricchio et al [11]. In both cases, the sealing skirt is obtained closing the struct cell geometries with several surfaces modelled at mid-thickness of the device frame. For the SAPIEN 3, the sealing skirt was modelled at crimped stage of TAVI and after the redo-TAVI for the Evolut PRO. Skirts were simulated using surfaces with triangular shell elements assuming thickness of 0.1 mm and were then connected to the device frames using tie contact conditions. Elastic-plastic material properties were assumed for sealing skirt materials [13]. To include the SAPIEN 3 valve leaflets after TAVI, we closed all cell-struct frame to mimic the leaflet displaced by the TAV-in-TAV. For the Evolut Pro, the device leaflets were mapped after redo-TAVI. Figure 1 shows the device models.

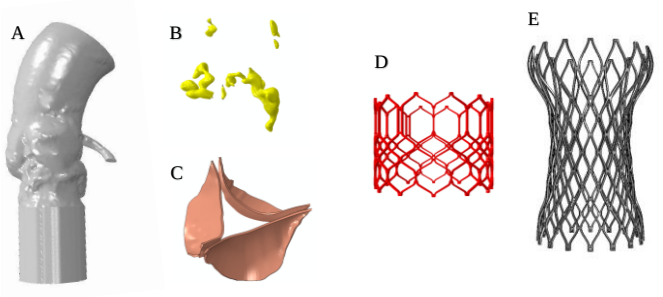

Figure 1: (A) patient model, (B) calcific plaques, (C) native valve leaflets, (D) SAPIEN 3 frame and (E) Evolut Pro frame

D. *Finite-element Analysis*

Numerical analysis of the redo-TAVI procedure was developed in Abaqus/Explicit (v2021hf7, Dassault Systèmes, USA) using a quasi-static approach and thus monitoring energy and ensuring the ratio of kinetic energy to internal energy remained less than 10%. Mass scaling was applied with an element-by-element stable time increment of 10^{-6} every 100 increments to reduce the computational cost.

The SAPIEN 3 stent frame was crimped by a rigid cylindrical surface gradually moved along the radial direction from the initial diameter of S3 (23 mm) to the final diameter of 6 mm. Frictionless contact condition was defined between the crimping surface and the device stent. Using a restart analysis, the crimped device was placed in the human host considering the stress state resulting from the crimping simulation (Fig. 2A). The SAPIEN device was positioned with an implantation depth of 5 mm. Expansion of S3 stent frame was simulated by the radial displacement of a rigid cylindrical surface representing the wall of the expanding balloon. The cylindrical surface is enlarged from the initial diameter of 6 mm to the nominal diameter of 23 mm. Frictionless contact was enabled between the cylindrical expanding surface and the S3 stent frame, which was allowed to be in contact with other anatomic parts. After expansion, an elastic recoil was allowed by the release of the cylindrical surface [5]. After TAVI simulation, the Evolut Pro was crimped using a cylindrical surface gradually moved along the radial direction from the initial device diameter to the final diameter of 6 mm using frictionless contact conditions. Both the stent and sleeve were positioned in the TAVI model with an implantation depth of 9 mm. By pulling the sleeve towards the distal ascending aorta and releasing the stent, because of its residual stresses, the Evolut Pro stent was gradually deployed into the TAV. The pull out of the rigid sleeve was performed by a uniform displacement of 75 mm.

Four different TAV-in-TAV scenarios were simulated varying the implantation depth or device size. The following parametric analysis were therefore performed:

1. 5-mm implantation depth for SAPIEN 3 and 9-mm implantation dept for Evolut Pro (reference configuration)
2. 5-mm implantation depth for SAPIEN 3 and 16-mm implantation dept for Evolut Pro (low redo-TAVI implantation depth)
3. 3-mm implantation depth for SAPIEN 3 and 9-mm implantation dept for Evolut Pro (high TAVI implantation depth)
4. 26-mm Evolut Pro in 23-mm SAPIEN 3 device (redo-TAVI overexpansion).

E. *TAV-in-TAV Analysis*

Eccentricity and expansion indexes were calculated from both TAVI CT and redo-TAVI CT images and then compared to those predicted by computational analysis. For each finite-element simulation the eccentricity index was calculated as follows: [1 − (minimum external THV diameter/maximum external THV diameter)] × 100 while the expansion index was expressed in relation to nominal prosthesis size as follows: (observed THV external area/ device area nominal size) × 100

[5]. Measurements were performed at 4 different anatomic levels (see Figure 6). For each simulation, the contact pressure exerted by the devices on the aortic wall was extracted. Distributions of contact pressure after redo-TAVI were mapped for the different scenarios.

III. Results

Comparison between numerical and CT-based structural indices showed that numerical expansion indices remain lower than CT measurement at different anatomic levels (ie, 120.8 ± 10% for CT-based measured of S3 versus 96.5 ± 14% for numerical-based measured of S3, while 90.6 ± 13% for CT-based measured of Evolut Pro versus 79.2 ± 21% for numerical-based measured of Evolut Pro). In a different way, the eccentricity index shows that numerical simulations slightly underestimates frame-related elliptical deformed shapes.

Figure 2 shows the delivering phases of SAPIEN 3 device and Mises stress distribution at the end of crimping phase. Similarly, Figure 3 displays the deployment of Evolut Pro in the previous SAPIEN 3 TAV as well as the Mises stress distribution for self-expandable device.

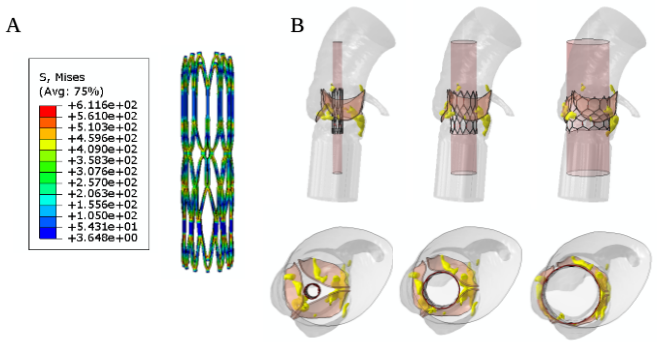

Figure 2 Deployment of SAPIEN 3 Ultra device simulating the TAVI

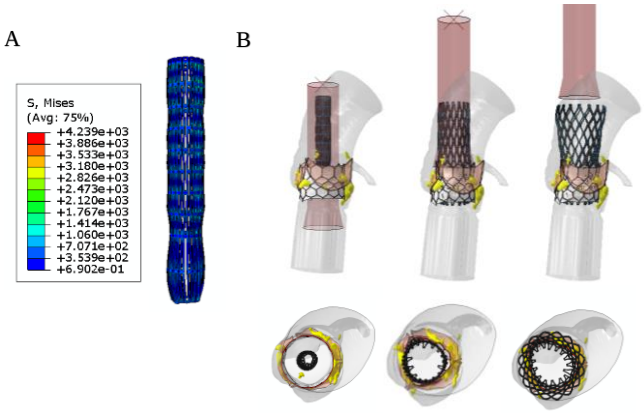

Figure 3 Deployment of Evolut Pro device simulating the redo-TAVI

Figure 4 illustrates the TAV-in-TAV deformed configurations for the four scenarios with different implantation depth or device overexpansion.

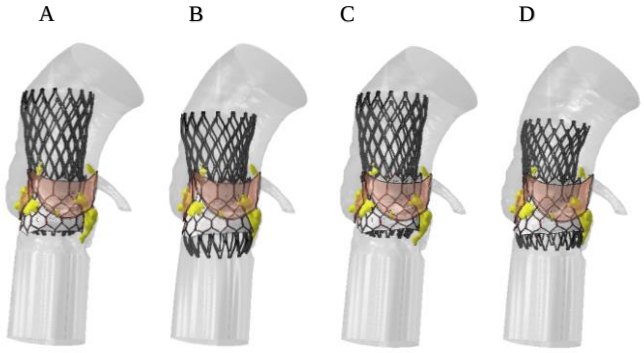

Figure 4 (A) reference TAV-in-TAV as done clinically, (B) low redo-TAVI, (C) high redo-TAVI and (D) TAV-in-TAV overexpansion

Figure 5 shows the Mises stress distribution and deformed shapes of each device.

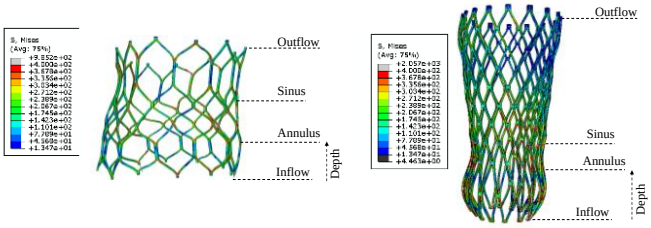

Figure 6: Mises stress distribution of each device for TAV-in-TAV

Figure 7 shows the contact pressure distribution for each TAV-in-TAV scenario.

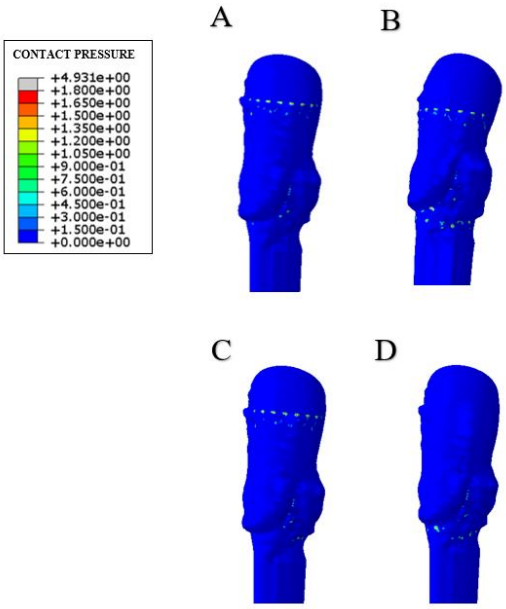

Figure 7 Contact pressure for (A) reference TAV-in-TAV as done clinically, (B) low redo-TAVI, (C) high redo-TAVI and (D) TAV-in-TAV overexpansion

IV. Discussion

To the best of our knowledge, this is the first computational study evaluating the structural mechanics of TAV-in-TAV. We first simulated the TAV-in-TAV according to the implantation depth and device size indicated by the Heart Team, and then carried out a parametric analysis varying these device parameters. The tendency of Evolut Pro devices to expand asymmetrically in the previous SAPIEN 3 device was observed and quantified at several anatomic levels. The utilize

of a larger device size than that used by the Heart teams has increased the contact pressure on the aortic wall. We also found that the high implantation depth of Evolut Pro can lead to a final skirt position likely closing the coronary ostia. Future computational flow studies will be undertaken to explore whether the parametrically-derived TAV-in-TAV shapes may lead to coronary flow obstruction and thus adverse events.

Computational analyses of the structural mechanics of TAVI demonstrated that an overexpansion of the implanted device can lead to a high risk of the aortic annulus rupture [9, 13-17]. The impact of aortic root anatomy and tilt angle of the device [18], calcification patterns [19] and native leaflet morphology [20] on the device deployment were also investigated. Fluid-solid interaction was also proposed to simultaneously simulate the structural mechanics and hemodynamics [21].

Moreover, simulations were used to explore the efficacy and safety of TAVI in young and high-risk patients, which are not conventionally treated with THVs. With regards to bicuspid patients, Brouwer et al. [22] carried out computational flow analyses to assess the paravalvular leakage in bicuspid patients, and thus demonstrate the feasibility of TAVI with the newest generation of THVs. Similarly, Pasta et al. [16] investigated stenotic bicuspid patients and found a good agreement between computer and post-TAVI CT-based measurements of the device conformation to the bicuspid anatomy.

Recently, the hemodynamic of TAV-in-TAV was investigated using particle image velocimetry by Hatoum and collaborators [23]. They performed a parametric analysis to investigate different device-size combination of TAV-in-TAV with both the SAPIEN 3 and Evolut THVs. They also found more turbulence for the TAV-in-TAV procedure as compared to that of traditional TAVI. In a different way, this study provided more insights on the structural mechanics of TAV-in-TAV to evaluate options for future indications when performing redo-TAVI.

V. Conclusion

We conclude that computational simulations can reveal important insights into the deployment of THVs when current devices experience structural valve failure. The outcome of TAV-in-TAV depends on both the original implant and the device to be implanted. Future flow studies are needed to assess whether the predicted TAV-in-TAV configurations can lead to coronary flow obstruction.

Acknowledgement

This project has received funding from the European Union's Horizon 2020 research and innovation programme under grant agreement No 101017523.

References

[1] Mylotte D, *et al.* Transcatheter heart valve failure: a systematic review. *Eur Heart J* 2015; 36(21): 1306-27.
[2] Arai T, *et al.* The feasibility of transcatheter aortic valve implantation using the Edwards SAPIEN 3 for patients with severe bicuspid aortic stenosis. *J Cardiol* 2017; 70(3-4): 220-24.
[3] Braghiroli J, *et al.* Transcatheter aortic valve replacement in low risk patients: a review of PARTNER 3 and Evolut low risk trials. *Cardiovascular diagnosis and therapy* 2020; 10(1): 59-71.
[4] Lifesciences E. 2015.
[5] Gallo M, *et al.* Transcatheter aortic valve replacement for structural degeneration of previously implanted transcatheter valves (TAVR-in-TAVR): a systematic review. *European Journal of Cardio-Thoracic Surgery* 2022; 61(5): 967-76.
[6] Ochiai T, *et al.* Risk of Coronary Obstruction Due to Sinus Sequestration in Redo Transcatheter Aortic Valve Replacement. *Jacc-Cardiovasc Inte* 2020; 13(22): 2617-27.
[7] Pasta S, *et al.* Three-dimensional parametric modeling of bicuspid aortopathy and comparison with computational flow predictions. *Artif Organs* 2017; 41(9): E92-E102.
[8] Pasta S, *et al.* Three-dimensional parametric modeling of bicuspid aortopathy and comparison with computational flow predictions. *Artif Organs* 2017.
[9] Scardulla F, *et al.* Shear stress alterations in the celiac trunk of patients with a continuous-flow left ventricular assist device as shown by in-silico and in-vitro flow analyses. *J Heart Lung Transplant* 2017; 36(8): 906-13.
[10] Di Giuseppe M, *et al.* Identification of circumferential regional heterogeneity of ascending thoracic aneurysmal aorta by biaxial mechanical testing. *J Mol Cell Cardiol* 2019; 130: 205-15.
[11] Cosentino F, *et al.* On the role of material properties in ascending thoracic aortic aneurysms. *Computers in biology and medicine* 2019; 109: 70-78.
[12] Bosi GM, *et al.* Population-specific material properties of the implantation site for transcatheter aortic valve replacement finite element simulations. *Journal of biomechanics* 2018; 71: 236-44.
[13] Pasta S, *et al.* Computational Analysis of Self-Expanding and Balloon-Expandable Transcatheter Heart Valves. *Biomechanics* 2021; 1(1): 43-52.
[14] La Grutta L, *et al.* TAVI imaging: over the echocardiography. *La radiologia medica* 2020: 1-19.
[15] Pasta S, *et al.* Transcatheter Heart Valve Implantation in Bicuspid Patients with Self-Expanding Device. *Bioengineering* 2021; 8(7): 91.
[16] Pasta S, *et al.* Simulation study of transcatheter heart valve implantation in patients with stenotic bicuspid aortic valve. *Med Biol Eng Comput* 2020.
[17] Pasta S, *et al.* Numerical simulation of transcatheter mitral valve replacement: The dynamic implication of LVOT obstruction in the valve-in-ring case. *Journal of Biomechanics* 2022; 144.
[18] Finotello A, *et al.* Finite element analysis of TAVI: Impact of native aortic root computational modeling strategies on simulation outcomes. *Medical Engineering & Physics* 2017; 47: 2-12.
[19] Sturla F, *et al.* Impact of different aortic valve calcification patterns on the outcome of transcatheter aortic valve implantation: A finite element study. *J Biomech* 2016; 49(12): 2520-30.
[20] Bailey J, *et al.* Assessing the impact of including leaflets in the simulation of TAVI deployment into a patient-specific aortic root. *Computer methods in biomechanics and biomedical engineering* 2016; 19(7): 733-44.
[21] Luraghi G, *et al.* The impact of calcification patterns in transcatheter aortic valve performance: a fluid-structure interaction analysis. *Computer methods in biomechanics and biomedical engineering* 2020: 1-9.
[22] Brouwer J, *et al.* Insight on patient specific computer modeling of transcatheter aortic valve implantation in patients with bicuspid aortic valve disease. *Catheter Cardiovasc Interv* 2018.
[23] Hatoum H, *et al.* The hemodynamics of transcatheter aortic valves in transcatheter aortic valves. *J Thorac Cardiovasc Surg* 2021; 161(2): 565-76 e2.